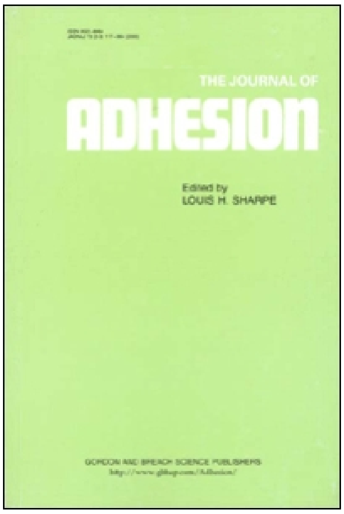

The Journal of Adhesion
Publication details, including instructions for authors and subscription information:
http://www.informaworld.com/smpp/title~content=t713453635

The Effects of Plasticity in Adhesive Fracture

Ming Du Chang[ab]; K. L. Devries[ac]; M. L. Williams[ac]
[a] College of Engineering. University of Utah, Salt Lake City, Utah, U.S.A. [b] Graduate Research Assistant Department of Mechanical Engineering, University of Utah, Salt Lake City, Utah, U.S.A. [c] College of Engineering, University of Utah, Salt Lake City, Utah, U.S.A.

To cite this Article Chang, Ming Du , Devries, K. L. and Williams, M. L.(1972) 'The Effects of Plasticity in Adhesive Fracture', The Journal of Adhesion, 4: 3, 221 — 231
To link to this Article: DOI: 10.1080/00218467208072225
URL: http://dx.doi.org/10.1080/00218467208072225

J. Adhesion, 1972, Vol. 4, pp. 221–231

The Effects of Plasticity in Adhesive Fracture†

MING DU CHANG‡ K. L. DEVRIES§ M. L. WILLIAMS§

College of Engineering, University of Utah,
Salt Lake City, Utah 84112 U.S.A.

(*Received November* 5, 1971)

From the viewpoint of continuum mechanics, and particularly the energy concept of fracture, adhesive and cohesive failures are similar. The essential difference involves the interpretation of the energy required to create new (adhesive or cohesive) surface area. This fracture mechanics approach has in the past been applied to a number of different elastic problems. In this investigation an elastic-perfectly plastic analysis for adhesive failure of a beam is presented. This analysis accounts for the energy dissipated during plastic bending. Experimental results with 6061-T6 alumimum are presented as evidence of the validity of the approach.

INTRODUCTION

Modern fracture mechanics began with the efforts of A. A. Griffith. In 1921 he presented a criteria for brittle fracture in elastic materials.[1] This criteria was based on a critical energy balance between the strain energy released and the energy required to create new surface area as the crack grows. According to this criteria, fracture is initiated at cracks (or other flaws) in the material. At such points the stresses are generally (mathematically) infinite even for small loadings. Griffith demonstrated that the integrated strain energy for an elastic plate including such "stress concentrations" remains finite, thereby circumventing the problem of infinite stresses. A balance between this energy and that required to form the fracture surface results in an equation of the

† This paper was presented at the *Symposium on Recent Advances in Adhesion* during the 162nd National American Chemical Society Meeting, September, 1971.

‡ Graduate Research Assistant, Department of Mechanical Engineering, University of Utah, Salt Lake City, Utah, U.S.A.

§ Professors, College of Engineering, University of Utah, Salt Lake City, Utah, U.S.A.

form, $\sigma_c = K(E\gamma_c/a)^{1/2}$. Where σ_c is the critical stress required for crack growth, K is a "geometric" factor depending on the exact flaw or crack shape and mode of loading, E is the modulus of elasticity, a is the flaw dimension, and γ_c is the specific fracture energy. The critical fracture stress is, therefore, seen to be a function of material properties (E and γ_c), the flaw size (a), and geometry. Later investigators have extended this original elastic analysis to include the effects of plastic and viscoelastic dissipation.[2,3]

Adhesive fracture mechanics is based on a similar rationale and energy balance. Recently M. L. Williams[4,5] and others[6] have discussed an essential similarity between cohesive and adhesive fracture. Physically the problems prove to be similar, differing only in the requirement to account for the difference in material properties on either side of the crack and the interpretation of the specific fracture energy. In the cohesive case the specific fracture energy, γ_c, is that required to create a unit of new fracture energy; in the adhesive case the specific adhesive fracture energy is the energy per unit area required to separate the two materials. Recent experiments[2-5] using a pressurized "blister test," various loaded beams and point-loaded circular plates strongly suggest that for "elastic" systems γ_a is a fundamental material constant. This paper presents preliminary efforts to analyze adhesive behavior including effects due to bending plasticity. Where plastic deformation occurs the energy balance must account for the energy dissipated as "plastic work" in those regions where the strains exceed those corresponding to the elastic limit.

In this study an energy balance is presented for end loaded cantilever beams. The analysis includes the effects of input work, stored strain energy, dissipated plastic energy, and specific adhesive surface energy.

ANALYSIS

The theoretical development is based on the usual assumptions of mechanics of materials:[8]

(1) The beam is composed of an isotropic, homogeneous, elastic perfectly plastic material.

(2) Yielding is governed by Von Mises criteria.

(3) Displacements are small.

(4) Plane sections remain plane.

From the assumptions listed above

$$\sigma_y = \sigma_z = \tau_{yz} = \tau_{xz} = 0, \qquad \sigma_x = \sigma, \qquad \tau_{xy} = \tau. \tag{1}$$

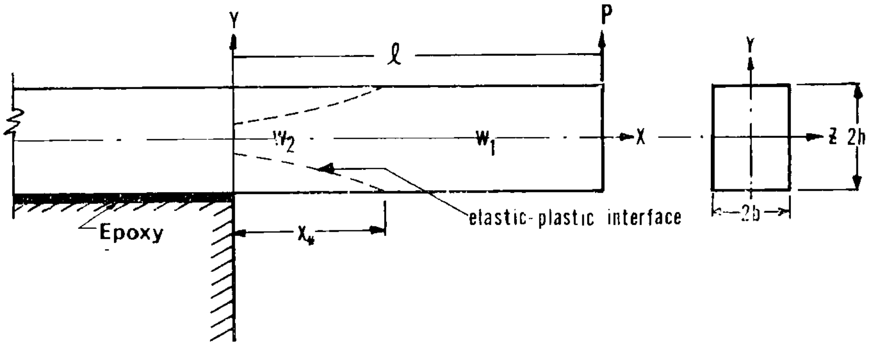

FIGURE 1 The geometry of the cantilever beam adhesive test specimen. x_* is the length over which plastic deformation occurs.

The components of the stress deviator are

$$S_x = \tfrac{2}{3}\sigma, \qquad S_y = S_z = -\tfrac{1}{3}\sigma. \tag{2}$$

The Von Mises yield criteria reduces to

$$\sigma^2 + 3\tau^2 = 3k^2 \tag{3}$$

where k is the yield stress in simple shear. If the shearing stress τ is zero, the constant k can be identified with normal tensile yielding at the tensile stress σ_0 so that

$$\sigma^2 \approx 3k^2 \tag{4}$$

Equation 3 can be written alternately as

$$\sigma^2 + 3\tau^2 = \sigma_0{}^2$$

For long slender beams it is reasonable to neglect vertical shear stress. Figure 2 shows the stress strain relationship for a beam of elastic-perfectly plastic material at strains exceeding the elastic limit.

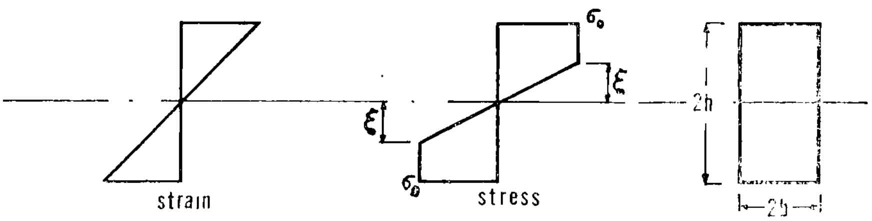

FIGURE 2 Strain and stress relationships for an elastic-plastic beam with a rectangular cross-section $2h \times 2b$.

In the leftmost part of the beam, i.e. the x_* region, the kinematics of deformation (4) is

$$\frac{d^2 w_2}{dx^2} = \frac{\sigma_0}{E\xi} \tag{5}$$

where w_2 is the displacement in the y-direction.

The moment in the elastic-plastic region is

$$M(x) = P(l - x) = \tfrac{2}{3}\sigma_0 b(3h^2 - \xi^2) \tag{6}$$

Solving Equation 6 for ξ

$$\xi = \sqrt{\frac{6\sigma_0 bh^2 - 3Pl + 3Px}{2\sigma_0 b}} \tag{7}$$

Substituting Equation 7 into Equation 5 results in

$$\frac{d^2 w_2}{dx^2} = \frac{\sqrt{2}b^{1/2}\sigma_0^{3/2}}{E\sqrt{6\sigma_0 bh^2 - 3Pl + 3Px}} \tag{8}$$

The boundary conditions for the idealized beam are:

$$\frac{dw_2}{dx} = 0 \quad \text{at} \quad x = 0$$

$$w_2 = 0 \quad \text{at} \quad x = 0 \tag{9}$$

From Equations 8 and 9

$$\frac{dw_2}{dx} = \frac{2\sqrt{2}b^{1/2}\sigma_0^{3/2}}{3PE}(\sqrt{6\sigma_0 bh^2 - 3Pl + 3Px} - \sqrt{6\sigma_0 bh^2 - 3Pl} \tag{10}$$

$$w_2 = \frac{2\sqrt{2}b^{1/2}\sigma_0^{3/2}}{3PE}\left[\frac{2}{9P}(6\sigma_0 bh^2 - 3Pl + 3Px)^{3/2} - (6\sigma_0 h^2 b - 3Pl)^{1/2}x - \frac{2}{9P}(6\sigma_0 bh^2 - 3Pl)^{3/2}\right] \tag{11}$$

In the elastic portion of the beam the kinematics of deformation from (4) is

$$\frac{d^2 w_1}{dx^2} = \frac{M}{EI} = \frac{P(l - x)}{EI} \tag{12}$$

from which

$$\frac{dw_1}{dx} = \frac{P}{EI}\left(lx - \frac{x^2}{2}\right) + c_1 \tag{13}$$

and

$$w_1 = \frac{P}{EI}\left(\frac{lx^2}{2} - \frac{x^3}{6}\right) + c_1 x + c_2 \tag{14}$$

From continuity at $x = x_*$

$$\left.\frac{\mathrm{d}w_1}{\mathrm{d}x}\right|_{x=x_*} = \left.\frac{\mathrm{d}w_2}{\mathrm{d}x}\right|_{x=x_*}$$

$$w_1\big|_{x=x_*} = w_1\big|_{x=x_*} \tag{15}$$

It will also be noted that

$$x_* = l - \frac{4}{3}\frac{\sigma_0 bh^2}{P} \tag{16}$$

From Equations 10, 11, and 13 through 16 it is possible to solve for c_1 and c_2. The resulting deflection at the free end is

$$\begin{aligned} w_1(l) = {} & \frac{Pl^3}{4bh^3E} + \frac{2\sqrt{2}\, b^{1/2}\sigma_0^{3/2}}{3PE}\left[\frac{2}{9P}(2\sigma_0 bh^2)^{3/2} - \frac{l}{3}(6\sigma_0 bh^2 - 3Pl)^{1/2}\right] \\ & - \frac{3P}{4bh^3E}\left(l - \frac{4}{3}\frac{\sigma_0 bh^2}{P}\right)^2\left(\frac{l}{3} + \frac{2}{9}\frac{\sigma_0 bh^2}{P}\right) \\ & + \frac{4}{3}\frac{\sigma_0 bh^2}{P}\left[\frac{2\sqrt{2}\, b^{1/2}\sigma_0^{3/2}}{3PE}\left(\sqrt{2\sigma_0 bh^2} - \sqrt{6\sigma_0 bh^2 - 3Pl}\right)\right. \\ & \left. - \frac{3P}{4Ebh^3}\left(\frac{l^2}{2} - \frac{8}{9}\frac{\sigma_0^2 b^2 h^4}{P^2}\right)\right] \end{aligned} \tag{17}$$

In the elastic region the strain energy can be separated into that due to volumetric strains and that due to strains associated with distortion of shape. If we assume incompressibility during plastic deformation, we need only consider the energy associated with distortion and the "constant" energy accumulated in these plastic regions up to the end of the elastic deformation.

In the elastic region the strain energy per unit volume is

$$\frac{\sigma_x{}^2}{2E} \tag{18}$$

The "constant" specific elastic energy accumulated up to the end of elastic deformation in the plastic zones is

$$\frac{\sigma_0{}^2}{2E} \tag{19}$$

The total strain energy V_2 is the sum of that stored in the elastic and plastic regions.

$$\begin{aligned} V_2 &= \int_{x_*}^{l} \int_{-h}^{h} 2b \frac{\sigma_x^2}{2E} \, dy \, dx + \int_{0}^{x_*} \int_{-\xi}^{+\xi} 2b \frac{\sigma_x^2}{2E} \, dy \, dx \\ &\quad + 2 \int_{0}^{x_*} \int_{\xi}^{h} (2b) \frac{\sigma_0^2}{2E} \, dy \, dx \\ &= -\frac{8}{27} \frac{\sigma_0^3 b^2 h^3}{EP} + \frac{2b\sigma_0^2 h}{E}\left(l - \frac{4}{3}\frac{\sigma_0 b h^2}{P}\right) \\ &\quad + \frac{4\sqrt{2}\, \sigma_0^{3/2} b^{1/2}}{27PE} (6\sigma_0 b h^2 - 3Pl)^{3/2} \end{aligned} \tag{20}$$

The energy dissipated during plastic distortion is given by

$$\begin{aligned} V_3 &= 4b \int_{0}^{x_*} \int_{\xi}^{h} \left(\frac{\sigma_0^2}{E\xi} y - \frac{\sigma_0^2}{E} \right) dy \, dx \\ &= \frac{4\sqrt{2}\, \sigma_0^{5/2} b^{3/2} h^2}{3PE} \left(\sqrt{2\sigma_0 b h^2} - \sqrt{6\sigma_0 b h^2 - 3Pl}\right) \\ &\quad - \frac{4b\sigma_0^2 h}{E}\left(l - \frac{4}{3}\frac{\sigma_0 b h^2}{P}\right) + \frac{2\sqrt{2}\, b^{1/2}\sigma_0^{3/2}}{9PE} \\ &\quad \times \left[(2\sigma_0 b h^2)^{3/2} - (6\sigma_0 b h^2 - 3Pl)^{3/2}\right] \end{aligned} \tag{12}$$

The in put work can be expressed in terms of the load, P, and the deflection $w_1(l)$

$$\begin{aligned} V_1 &= \int_0^{w_1(l)} P(y) \, dy \\ \frac{\partial V_1}{\partial l} &= P \frac{\partial w_1(l)}{\partial l} \end{aligned} \tag{22}$$

For conservation of energy

$$\frac{\partial V_1}{\partial l} = \frac{\partial V_2}{\partial l} + \frac{\partial V_3}{\partial l} + 2b\gamma_a \tag{23}$$

where l is total length of beam including the crack length. Making appropriate substitutions:

$$\begin{aligned} \gamma_a = \frac{1}{2b} \Bigg[& \frac{\sqrt{2}\, b^{1/2}\sigma_0^{3/2} Pl}{3E\sqrt{6\sigma_0 b h^2 - 3Pl}} - \frac{2\sqrt{2}\, \sigma_0^{5/2} b^{3/2} h^2}{3E\sqrt{6\sigma_0 b h^2 - 3Pl}} \\ & - \frac{5\sqrt{2}\, b^{1/2}\sigma_0^{3/2}}{9E} \sqrt{6\sigma_0 b h^2 - 3Pl} + \frac{2b\sigma_0^2 h}{E} \Bigg] \quad \text{(for plane stress)} \end{aligned} \tag{24}$$

Strictly speaking Equation 24 is valid only for those loadings sufficient to cause plastic deformation in the beam but insufficient to produce a "plastic hinge" at the supported end. That is Equation 24 is valid for the regime

$$2\sigma_0 bh^2 > Pl \geq \tfrac{4}{3}\sigma_0 bh^2 \tag{25}$$

Elastic analysis is valid for the regime

$$Pl \leq \tfrac{4}{3}\sigma_0 bh^2$$

In which case

$$\gamma_{ae} = \frac{3}{16}\frac{P^2l^2}{Eb^2h^3} \tag{25a}$$

It should be noted that the proceeding analysis has been for plane stress, e.g. a narrow beam. The solution to the plane strain problem, e.g. a plate or a beam with greater width than depth, can be obtained by multiplying the strain energy in the above equations by the factor $(1 - \nu^2)$ where ν is Poisson's ratio for the elastic portions of the analysis and assuming incompressibility during plastic deformation ν is equal to $\frac{1}{2}$ in the dissipative regimes. Making these substitutions

$$\gamma_a = \frac{1}{2b}\left[\frac{\sqrt{2}\,(1 - v^2)b^{1/2}\sigma_0^{3/2}\cdot Pl}{3E\sqrt{6\sigma_0 bh^2 - 3Pl}} - \frac{\sqrt{2}\,(1 + 8v^2)\sigma_0^{5/2}b^{3/2}h^2}{6E\sqrt{6\sigma_0 bh^2 - 3Pl}} - \frac{11\sqrt{2} + 16\sqrt{2}\,v^2}{36E}\sqrt{6\sigma_0 bh^2 - 3Pl}\,b^{1/2}\sigma_0^{3/2} + \frac{(1 + 2v^2)\sigma_0^{\,2}bh}{E}\right]$$

for plane strain (26)

Equation 26 is valid for the regime

$$2\sigma_0 bh^2 > Pl \geq \tfrac{4}{3}\sigma_0 bh^2$$

An appreciation for the size of these plastic effects can be obtained by defining an apparent plastic specific fracture energy term as

$\Delta E = \gamma_a - \gamma_{ae}$ (for plane strain)

$$\Delta E = \frac{1}{2b}\left[\frac{\sqrt{2}\,(1 - v^2)b^{1/2}\sigma_0^{3/2}Pl}{3E\sqrt{6\sigma_0 bh^2 - 3Pl}} - \frac{\sqrt{2}\,(1 + 8v^2)\sigma_0^{5/2}b^{3/2}h^2}{6E\sqrt{6\sigma_0 bh^2 - 3Pl}} - \frac{(11\sqrt{2} + 16\sqrt{2}\,v^2)b^{1/2}\sigma_0^{3/2}}{36E(6\sigma_0 bh^2 - 3Pl)^{-1/2}} + \frac{(1 + 2v^2)\sigma_0^{\,2}bh}{E}\right] - \frac{3(1 - v^2)P^2l^2}{16Eb^2h^3} \tag{27}$$

A plastic dissipation parameter might be defined as:

$$\Delta V_3 = Pl - \tfrac{4}{3}\sigma_0 bh^2 \tag{28}$$

ΔE plotted in Figure 3 indicates the greater the plastic dissipation, the larger the effect of plastic deformation on the specific adhesive fracture

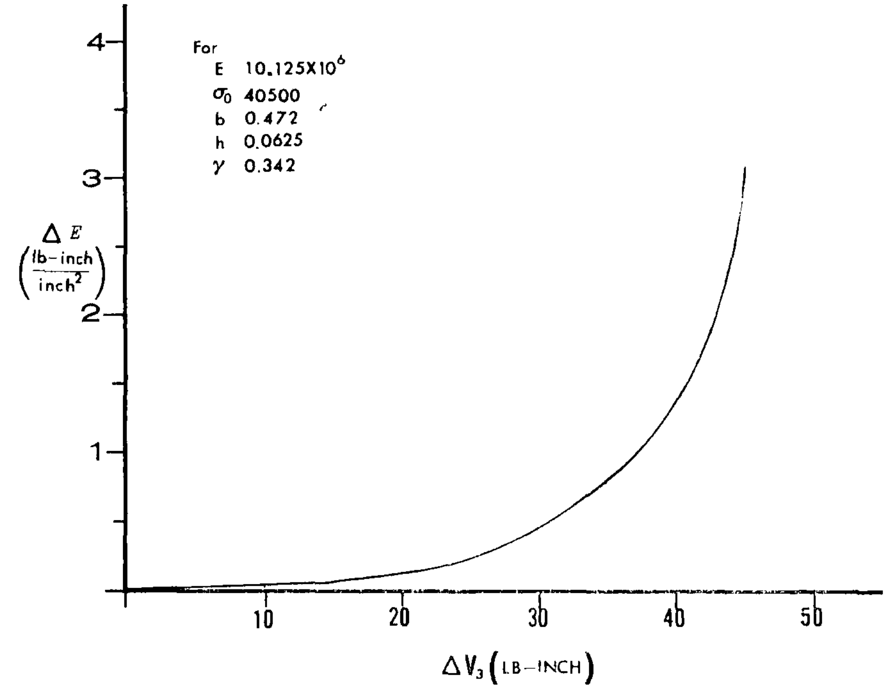

FIGURE 3 $\gamma_a - \gamma_{ae}$ versus the plastic deformation parameter.

energy (γ_a). Note that as the conditions for a plastic hinge are approached, i.e. $Pl \to 2\sigma_0 bh^2$ the dissipation increment, ΔE, becomes very large as would be expected.

EXPERIMENTAL PROCEDURES AND RESULTS

Experiments were planned and conducted to confirm the above analysis. The experiments were conducted on beams of 6061-T6 aluminum. This material was chosen because experimentally it very nearly obeys the elastic-perfectly plastic behavior assumed in the analysis. Experimentally this material was found to have a Young's modulus of 10.125×10^6 psi and a yield point of 4.05×10^4 psi. Bonding was accomplished with a structural adhesive (3M Company—2216 B/A) that had a low concentration of volatiles and hardened at room temperature. Surfaces were prepared for bonding by carefully sanding with wet 400A paper and cleaning with acetone. Care was taken to uniformly mix and apply the adhesive. Thickness of the adhesive film was controlled by a single thickness of Temp-R-Tape (self-adhering, 6 mils thick) used as a spacer at the "crack" portion of the cantilever as shown in Figure 4. This tape also served to give a reproducible crack geometry.

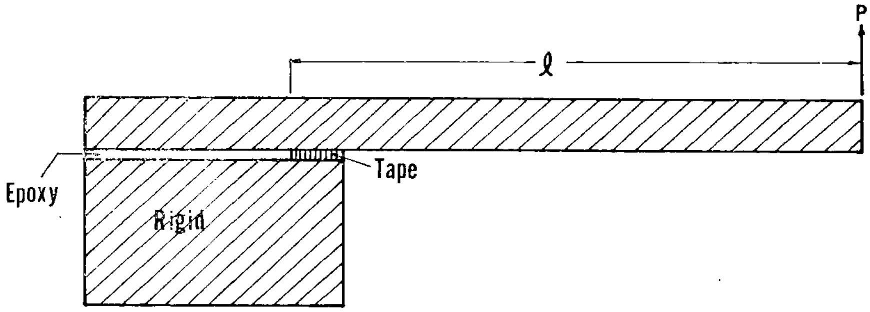

FIGURE 4 Cantilever beam experimental geometry for elastic-plastic investigation.

The sample was cured 75 hours before testing. The load was increased at a uniform rate until failure with the aid of a servo-controlled loading system with load feedback. The fracture originated at the tape spacer. Failure was catastrophic in nature in that the linearly increasing load up to the failure point dropped "instantaneously" to zero. Optically the fracture appeared to be largely adhesive in nature with the crack occurring on the beam and base side of the adhesive with approximately equal probability.

The upper plate was $\frac{1}{8}$ inch thick, $\frac{15}{16}$ inches wide, and nine inches long. The base (assumed rigid in the analysis) was $\frac{1}{2}$-inch thick, $1\frac{1}{2}$ inches wide, and several inches long. The adhesive part of the surface was $2\frac{1}{2}$ inches long. Experimentally the cantilever length, l, was varied from three to six inches. The resulting loads fell in the range of twenty to forty pounds. The length and loads studied fell in the range, satisfying the inequality expressed on the left-hand side of Equation 25. As a result plastic "hinges" were not formed during testing.

For the fracture mechanics approach to have meaning and be useful, the energy required per unit area of crack growth must be constant. Figure 5 shows the adhesive fracture load as a function of the cantilever beam length l. The general trend of this curve is in agreement with Equation 26. Figure 6 shows γ_a as a function of L including the effect of plasticity in the analysis (Equation 26). Here γ_a is constant within experimental error and can be

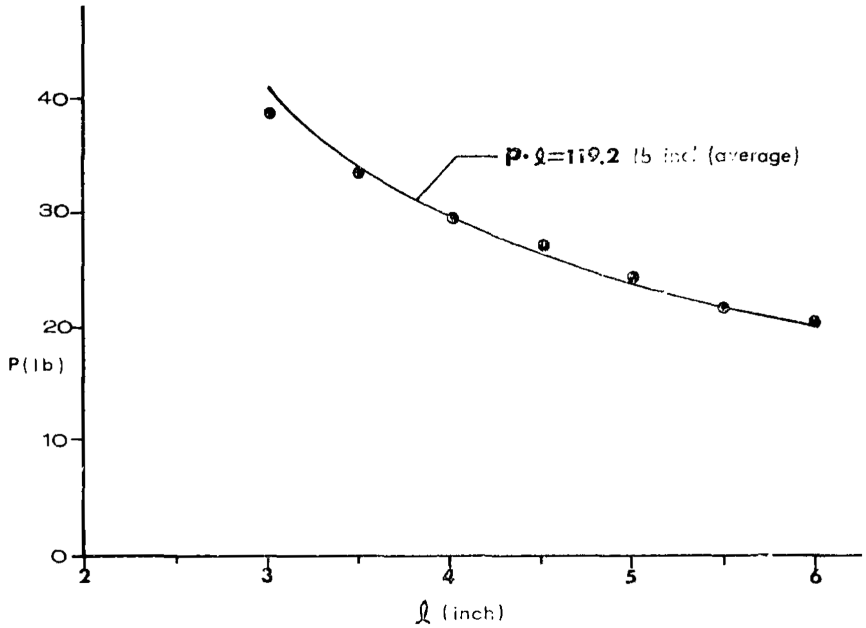

FIGURE 5 Critical load versus length l for the cantilever member in the elastic-plastic deformation.

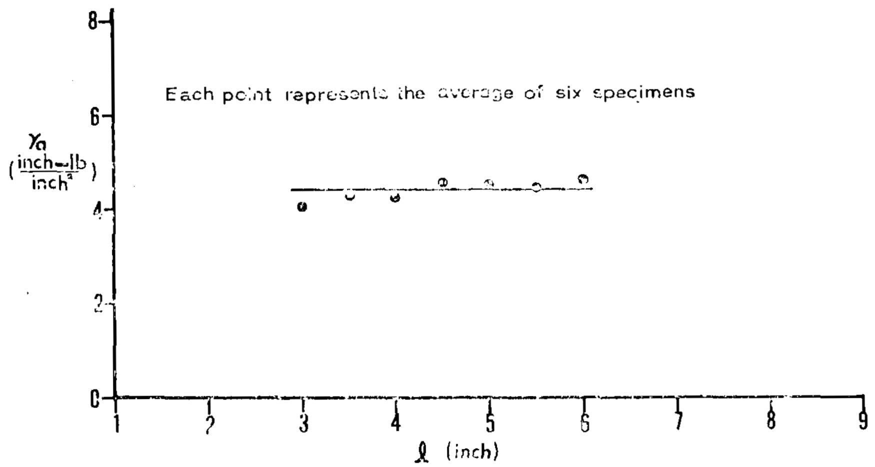

FIGURE 6 Adhesive surface energy versus length l for the cantilever member accounting for bending plastic dissipation.

viewed as a material property. The line in Figure 6 represents the average of all tests. The very slight increase in γ_a with l apparent in this figure is attributed to a small amount of work hardening in the aluminum samples.

DISCUSSION AND CONCLUSIONS

When "all the energy terms" are included in the thermodynamic energy balance, the adhesive fracture energy is essentially constant at a value of $\sim$4.35 inch-lbs/inches^2 (7.81 $\times$ 10^5 ergs/cm^2). This is interpreted as evidence that an energy balance including plasticity is a valid failure criteria for adhesive fracture. Some caution must be exercised in interpreting just which plasticity effects are included in the analysis presented here. Only the effects of the "bending" plasticity in the aluminum beam are included. Some plasticity could occur in the epoxy cement used as the adhesive agent. Indeed the rather high value determined for γ_a would indicate that some dissipation mechanisms are present. The energy required to break the "back-bone" polymeric bonds required to form a square centimeter of new surface can be estimated as not to exceed a few hundred ergs/cm^2. The remainder of the energy must be due to viscoelasticity, plasticity, secondary bond rupture, etc. at the tip of the progressing crack. These effects in the epoxy are all lumped into the γ_a term, a not uncommon practice in cohesive fracture mechanics.[7] It appears the analysis and experimental results reported here do confirm that it is possible to account analytically for the gross effects of plasticity in adhesive fracture. We are confident that the analysis can be extended to more complex geometries.

References

1. A. A. Griffith, *Proceedings of the First Congress of Applied Mechanics*, Delft. 1924, p. 55.
2. A. S. Tetelman and A. J. McEvily, *Fracture of Structural Materials* (John Wiley and Sons, Inc., New York, 1967).
3. M. L. Williams, *Fundamental Phenomena in the Materials Sciences*. (Plenum Press, New York, 1967), Vol. 4, p. 23.
4. M. L. Williams, *Journal of Applied Polymer Science* **13**, 29 (1969).
5. M. L. Williams, *Journal of Applied Polymer Science* **14**, 1121 (1970).
6. B. M. Malyshev and R. L. Salganik, *International Journal of Fracture Mechanics* **1**, 114 (1965).
7. J. J. G. Iman, *Journal of Applied Physics* **31**, 2208 (1960).
8. A. Mendelson, *Plasticity*. (Macmillan Publishing Company, New York, 1968).
9. E. Orowan, *Welding Research Supplement* **20**, 57 (1955).

Acknowledgements

The research reported herein was supported by the National and Aeronautics and Space Administration, Contract No. NGL 45-003-029.